Available online at www.sciencedirect.com
ScienceDirect
Ceramics International 38 (2012) 141–146
CERAMICS INTERNATIONAL
www.elsevier.com/locate/ceramint

Enhanced mechanical and dielectric behavior of $BaTiO_3$/Cu composites

Xu Ning [a,b,*], Pu Yongping [a], Wang Bo [a], Wu Haidong [a], Chen Kai [a]

[a] School of Materials Science and Engineering, Shaanxi University of Science & Technology, Xi'an 710021, China
[b] Key Laboratory of Auxiliary Chemistry & Technology for Chemical Industry, Ministry of Education, Shaanxi University of Science & Technology, Xi'an 710021, China

Received 18 May 2011; received in revised form 24 June 2011; accepted 24 June 2011
Available online 2nd July 2011

Abstract

$BaTiO_3/x$Cu composite ceramics with $x = 0$–30 wt.% were fabricated by the traditional mixing method in nitrogen gas. The mechanical properties and electric properties of the obtained composites were investigated as a function of the Cu mass fraction using a three bending test and impedance spectroscopy. The results indicated that the relative density of the sintered composites reached above 91%, the Cu-dispersed $BaTiO_3$ composites enhanced the mechanical properties, particularly the high fracture toughness (~3.9 MPa $m^{1/2}$) and bending strength (~134 MPa), compared to the monolithic $BaTiO_3$. Furthermore, the percolation threshold of $BaTiO_3$/Cu composites was $x = 25$ wt.%. The permittivity (ε_r) markedly increased from ~2000 for monolithic $BaTiO_3$ to ~9000 with increasing Cu up to 30 wt.%. Additionally, the temperature coefficient of this system was less than 5% in the temperature range of 25–115.

Key words : C. Mechanical properties; C. Electrical properties; $BaTiO_3$/Cu composites

1. Introduction

The influences of metallic phases in ferroelectric and paraelectric materials have been investigated for various combinations such as $BaTiO_3$/Ag [1], PZT/Pt [2], $BaTiO_3$/Ni [3], $BaTiO_3$/Cr [4] and $SrTiO_3$/Pt systems [5], which typically show very high mechanical properties, dielectric constants and have been of special interest for applications related to energy storage. Hwang [6] has reported that the internal stress of ceramic/metal composites produced during the sintering could be effectively relaxed due to plasticity of the metal, and Carlos Pecharroman et al. [7] has got the similar conclusions in studying the Ni/BT composites. Chen and Tuan [8] have reported that the role of Ag in the sintering and grain growth of the BT/Ag composites, and the mechanical properties and dielectric properties when the particle size is blow 10 μm. The results show that the metallic phase acts as a bridge within the ceramic and not only improves the mechanical properties, such as preventing crack propagation and increasing the bending strength, fracture toughness and the strength of the matrix [9–11], but, according to the percolation phenomenon [12], also changes the electrical properties of the matrix, such as the piezoelectric properties, permittivity (ε_r) and electrical conductivity. However, it has been very difficult to experimentally observe the phenomena occurring at the percolation threshold, and only a few groups have reported the effect of a strongly enhanced permittivity for ceramic–metal composites in the neighborhood of the percolation threshold [13,14].

A dielectric characteristic study of the ceramic–metal composites indicated that the composite's response to an applied electric field may be attributed to different types of polarization, which may be affected by varying the temperature or the electric field frequency [2]. Some large ε_r ferroelectric $BaTiO_3$ ceramics could be obtained through doping with Pt, Ag or other noble metals.

In this paper, the effects of the addition of Cu as the metallic phase to $BaTiO_3$ on the sintering properties and dielectric characteristics were studied. To protect Cu from being oxidized during the sintering, it was necessary to sinter the composite in a reducing atmosphere.

* Corresponding author at: School of Materials Science and Engineering, Shaanxi University of Science & Technology, Xi'an 710021, China.
Tel.: +86 29 86168803; fax: +86 29 86168688.
E-mail address: xu-ning-skd@163.com (Xu. Ning).

0272-8842/$36.00
doi:10.1016/j.ceramint.2011.06.048

2. Experimental procedure

The raw materials were commercially available barium titanate powders ($BaTiO_3$, purity: 99.9%, average particle size: 0.45 μm, Fenghua Advanced Technology, China) synthesized by a hydrothermal method and copper powders (Cu, purity: 99.8%, average particle size: 74 μm, Zhengzhou Chemical Reagent, China). First, the $BaTiO_3$ and Cu powders were mixed with copper content of 0, 5, 10, 15, 20, 25, 30 wt.% by ball milling with ethanol in a resin container for 4 h. Then, the slurry was dried, pulverized and sieved with a 150 μm mesh. Next, green compacts of 14 mm in diameter and 2 mm in thickness were formed by a stainless steel mold with 5 MPa for 3 min. The samples were sintered at 1290 °C, 1300 °C and 1320 °C °C in N_2 flow for 2 h using a heating rate of 3 °C/min.

Density measurements of the sintered samples were carried out on the basis of the Archimedes principle by immersing sintered compacts in water and determining the samples' volume by their volume displacement. X-ray diffraction (XRD, Cu Ka, diffraction angle: 15°–60°, angular step interval: 0.02°, Model: D/max2200pc, 2002, Rigaku, Tokyo, Japan) was used to identify the phase regarding the sintered composite discs, and the microstructure characterization of composite discs was carried out using a scanning electron microscope (SEM, Model: JEOL JSM-6390A JEOL Ltd., Tokyo, Japan). To visualize the element distributions of Ba, Ti, and Cu, analytical SEM by energy-dispersive X-ray spectroscopy (EDS) was performed on the composites.

The bending strength and fracture toughness were measured by three-point bending with loading spans of 14 mm at a cross-head speed of 0.5 mm/min on a small rectangular block specimen (4 mm × 5 mm × 20 mm) with one well-polished surface and single-edge notched beam specimens with a notch depth of 1 mm by a PC—1036PC tester at room temperature.

Before applying electrodes for dielectric measurements, the top and bottom surface layers of the compacted composites were removed through grinding with SiC paper. Finally, the prepared samples were coated with In–Ga as the electrodes for measuring of electric properties. The resistance, dielectric loss and frequency dependence of permittivity with different copper content were evaluated in frequency range 10^2–10^6 Hz using the Agilent impedance analyzer (Model: E4980A, Agilent Tech., CA, USA). The temperature dependence of permittivity was carried out on the electric field of 1 V/mm (Model: HP4284A, Agilent Tech., CA, USA) from room temperature to 160 °C at a heating rate of 2 °C/min.

3. Results and discussion

The XRD patterns of $BaTiO_3$/Cu composites sintered at 1290 °C are shown in Fig. 1. All peaks were attributed to either the $BaTiO_3$ phase or Cu without any impurities being observed, suggesting that no reaction took place between $BaTiO_3$ and Cu during the sintering. Further more, the diffraction peaks of $BaTiO_3$ in the composites did not shift, indicating that the copper was not incorporated in the perovskite structure [15,16]. As expected the relative diffraction intensities of the Cu

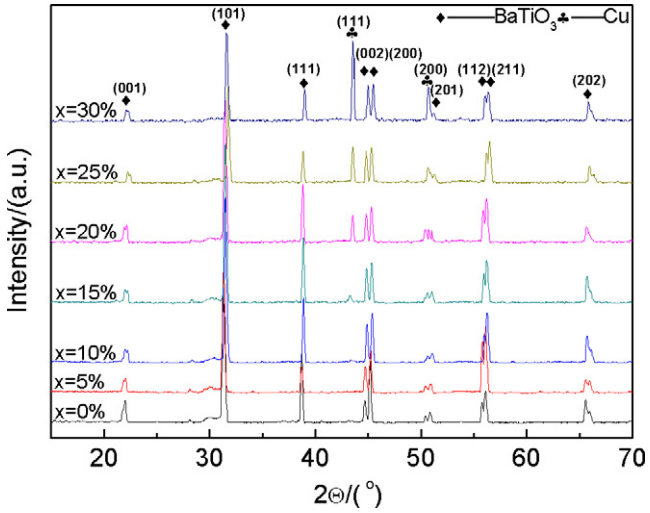

Fig. 1. X-ray diffraction patterns of $BaTiO_3$/xCu composites sintered at 1290 °C in N_2 flow for 2 h.

reflections compared to the ones of $BaTiO_3$ increased with the increase of Cu content. The evolution of the XRD-peaks confirms the successful composition control during sintering.

Fig. 2 shows the relative density of $BaTiO_3$/Cu composites sintered at 1290 °C, 1300 °C and 1320 °C. The relative densities of the compacts were larger than 91% for all compositions. The relative density of the composites increased to a maximum value of 97.7% ($x = 0$) sintered at 1300 °C and then decreased with increasing of sintering temperature and Cu content. From the standpoint of optimum density, the sintering temperature of 1300 °C can be regarded as a critical value, which is consistent with our bending strength and fracture toughness measurements. It was considered that there were a small amount of macro-bubbles that appeared between the different phases due to the emergence of the Cu liquid phase during sintering with the introduction of metal particles into a matrix of $BaTiO_3$, which reduced the interconnection between $BaTiO_3$. It was still possible that the decrease in density was caused by pores formed during cooling process.

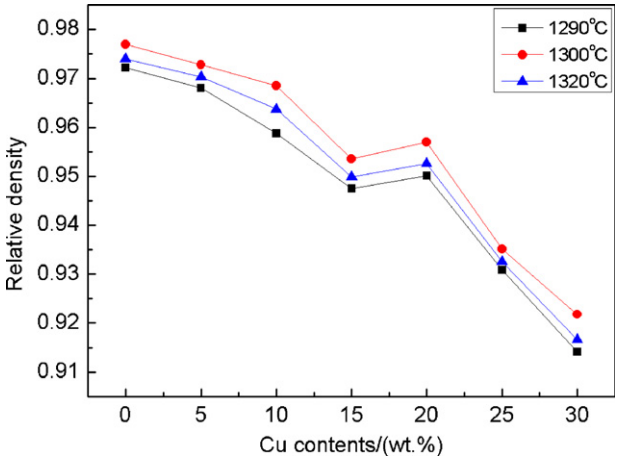

Fig. 2. Relative density of $BaTiO_3$/Cu composites sintered in N_2 flow at 1290 °C, 1300 °C and 1320 °C for 2 h.

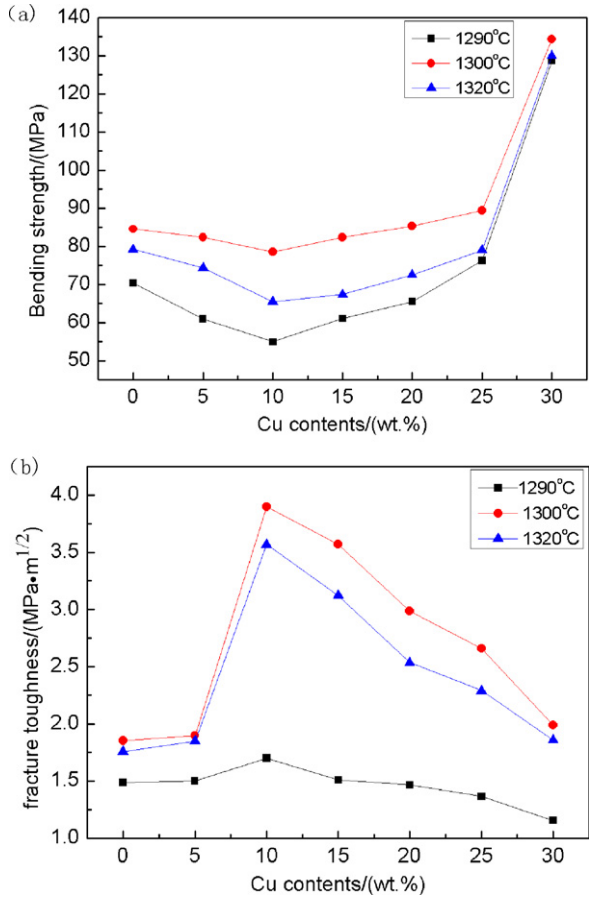

Fig. 3. Bending strength (a) and fracture toughness (b) of $BaTiO_3$/Cu composites sintered in N_2 flow at 1290 °C, 1300 °C and 1320 °C, respectively.

The bending strength and fracture toughness of $BaTiO_3$/Cu composites sintered in N_2 flow at 1290 °C, 1300 °C and 1320 °C are shown in Fig. 3. The bending strength, σ, was determined from [17]

$$\sigma = \frac{3PL}{2BW^2} \tag{1}$$

where P is the fracture load, L is the loading span in the three-point bending test, and B and W are the width and thickness of the specimen, respectively. The fracture toughness, K_{IC}, was calculated from the following formula [17]

$$K_{IC} = Y\frac{3PL}{2\sqrt{1000}BW^2}\sqrt{a} \tag{2}$$

where P, L, B, and W are the same as Eq. (1) and Y is a function of the ratio of notch length (a) and specimen thickness (W) given by

$$Y = 1.93 - 3.07\left(\frac{a}{W}\right) + 14.53\left(\frac{a}{W}\right)^2 - 25.07\left(\frac{a}{W}\right)^3 + 25.8\left(\frac{a}{W}\right)^4 \tag{3}$$

It can be seen from Fig. 3 that the bending strength of the composites decreased slightly with increasing copper content in the range of x from 0 to 25 wt.% and had a abrupt change of x from 25 to 30 wt.%; and the fracture toughness of the composites increased to a maximum value of 3.9 MPa $m^{1/2}$ up to 10 wt.% of Cu addition. It can also be seen from the figure that mechanical properties of the composite reached the optimum performance when sintered at 1300 °C, which had the similar variation trend with relative density of the composite with sintering temperature.

The bending strength reached to a maximum value of 134.4 MPa for 30 wt.% of Cu addition, which was 1.6 times larger than that of the monolithic $BaTiO_3$ prepared under the same conditions. The bending strength of a compound is heavily dependent on its material composition, grain size and porosity. The Ryskewitsch formula [18] demonstrates this relation well:

$$\sigma = \sigma_o \exp(-np) \tag{4}$$

where σ_o is the strength of the dense body, n is a constant between 4 and 7, and p is the porosity. It is clear that the bending strength decreases with increasing of the porosity almost exponentially, and falls to half of the free pore ones when p is 10%. That is why there was a decreasing of bending strength with increasing copper content from x = 0 wt.% to x = 10 wt.%. However, with the introduction of metal particles into a matrix of $BaTiO_3$, the energy released from the crack propagation was absorbed by the plastic deformation of the metal and stopped the formation of the micro-cracks at the phase boundary, as suggested by the Griffith's micro-cracks theory [19]. Therefore, a gradually increase of the bending strength above 10 wt.% of Cu addition and a drastic increase of that around x = 25 wt.% were observed. This can also be interpreted as the interpenetrating network produced during introduction of copper into $BaTiO_3$ matrix as shown in Fig. 4 the SEM of cross section (a) and local enlarged drawing of copper particles (b) in the $BaTiO_3$/xCu composites with x = 10 wt.%. It can be seen from Fig. 4(a) that the copper flakes with a diameter of 25 μm and thickness of 2 μm arranged in the $BaTiO_3$ matrix randomly. Konopka et al. also showed that the interpenetrating network is found in Al_2O_3/Fe systems and the network changes the mechanical properties of the composites [28]. The interface between $BaTiO_3$ and Cu gives an opportunity to develop an interpenetrating network with a strong ceramic–metal bonding, thus increasing the bending strength of the matrix greatly.

As seen in Fig. 3(b), the fracture toughness reached to the peak value up to 10 wt.% Cu addition and then decrease above x = 10 wt.%. These changes in fracture toughness were thought to be due to oxygen vacancies caused during sintering in a nitrogen atmosphere [20,21]. The Cu–O bond at the interface between $BaTiO_3$ and Cu reduced with decreasing the concentration of oxygen, which lead to the decline in fracture toughness.

The conductivity of $BaTiO_3$/Cu composites as a function of Cu content is shown in Fig. 5. When x = 5 wt%, the conductivity was $\sim 7.4 \times 10^{-4}$ S/m, and the percolation threshold, which is denoted by a nonlinear transition, occurred when x = 25 wt.%. At 20 wt.% of Cu addition, the conductivity of the composites has a sharp increase to $\sim 7.9 \times 10^{-3}$ S/m and

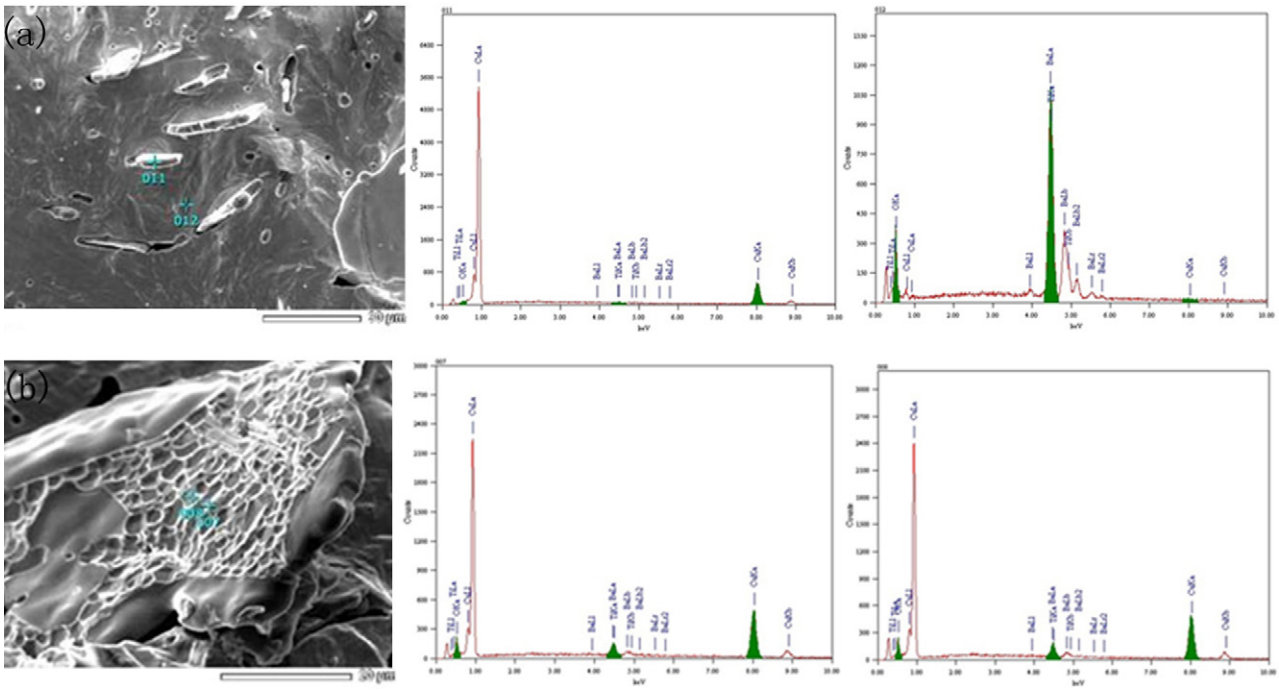

Fig. 4. SEM of cross section (a) and local enlarged drawing of copper particles (b) in the $BaTiO_3/x$Cu composites (x = 10 wt.%) sintered at 1290 °C in N_2 flow.

continued to increase but at a slower rate above x = 25 wt%, which could be explained by the percolation phenomenon and the diagram of the conductivity model in Fig. 5. According to the percolation theory [22,23]

$$\sigma \propto \sigma_M (f - f_c)^t \quad f > f_c \tag{5}$$

$$\sigma \propto \sigma_D (f_c - f)^{-q} \quad f < f_c \tag{6}$$

where σ, σ_M, σ_D are the conductivity of composite materials, conductors and insulators (dielectric), respectively, f_c is the percolation threshold, and t and q are the critical exponents though there has not yet a unified understanding about the critical indices' values in academia. Still, the resistivity of the

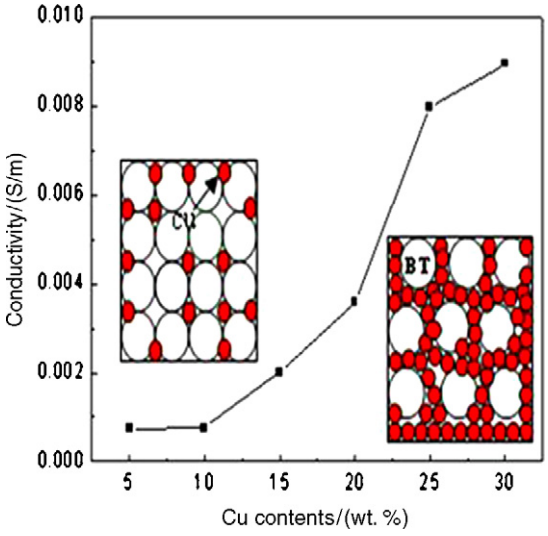

Fig. 5. Conductivity of $BaTiO_3$/Cu composites sintered at 1290 °C in N_2 flow.

$BaTiO_3$/Cu composites followed formula (5) when the copper content was lower than percolation threshold ($f < f_c$), and the resistivity was close to that of the insulator due to the dispersed of conductive particles into the matrix in clusters as shown in the model on the left in Fig. 5. Additionally, when the amount of Cu was higher than percolation threshold ($f > f_c$), as described by formula (6), the conductive particles gathered into larger clusters and interconnected into an infinite cluster. When the content of Cu reached the critical value, it formed a conductive pathway as shown in the model on the right of Fig. 5.

Fig. 6 shows the permittivity of $BaTiO_3$/Cu composites with different Cu content as a function of the frequency (a) of the applied electric field and temperature (b). As shown in Fig. 6(a), the permittivity increased with increasing Cu content and attained a value of ~3000 when x = 5 wt.% and ~9000 when x = 30 wt.% at 1 kHz. Furthermore, the variation in permittivity decreased distinctly from 200 Hz to 2 MHz. This variation of permittivity is due to changes in the four basic mechanisms which affect the polarization, α_t; the mechanisms, in the order of their response times, are the electronic polarization [α_e], ionic polarization [α_i], dipolar polarization [α_o] and the space charge [α_s]. These yield the following system [24–27]:

$$\alpha_t = \alpha_e + \alpha_i + \alpha_o + \alpha_s \tag{7}$$

Each of these polarization mechanisms has its own intrinsic response time and natural frequency. While the electronic polarization [α_e] is active at atomic vibrations and optical frequencies and beyond, ionic polarization [α_i] is affected at infrared frequencies (~10^{13} Hz). The space charge [α_s] mechanism could require some time to build up and, therefore, corresponds to fractions of a kHz. The space charge mechanism has an important role in this system, because there are many

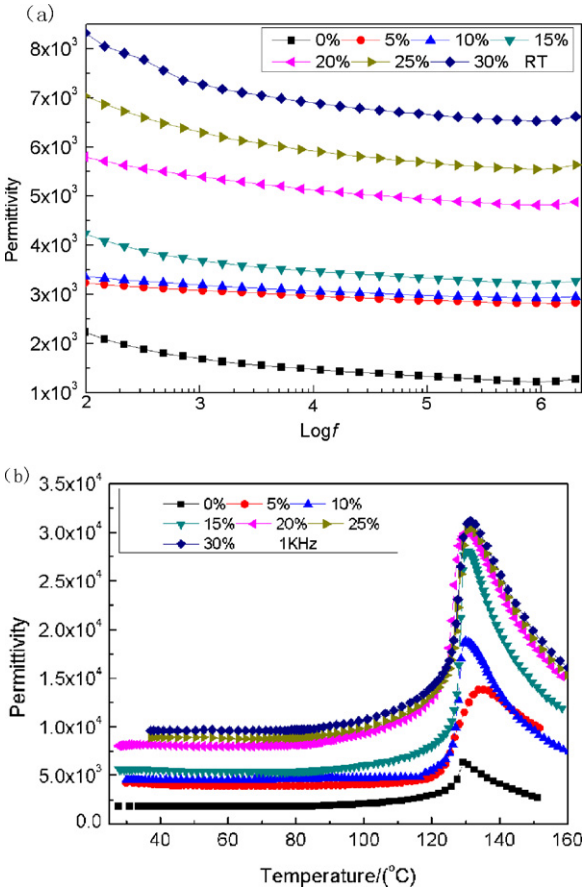

Fig. 6. Dependence of permittivity of $BaTiO_3$/Cu composites on frequency (a) and temperature (b) sintered at 1290 °C in N_2 flow.

space charges generated between $BaTiO_3$ and Cu, and the quantity of space charges rise with the increase of amount of Cu. Consequently, the permittivity of $BaTiO_3$/Cu composites increased significantly with increasing Cu content, and the maximum value was ~9000 when $x = 30$ wt.% at 1 kHz. This large increase in permittivity at the lower frequencies was mainly attributed to polarization caused by the space charge mechanism. When the applied frequency was much higher than the natural frequency of the dipole, the dipole was not able to react and consequently did not contribute to the permittivity.

The variation in the permittivity from room temperature (25 °C) to the peak temperature (130 °C) was 3.6×10^4 when $x = 30$ wt.%, as shown in Fig. 6(b). It can be seen that the Curie peak did not shift and consistent with that of monolithic $BaTiO_3$, which also proved that the copper was not incorporated in the perovskite structure. Below the Tc (130 °C), the permittivity was very stable until the temperature reached approximately 115 °C, the temperature coefficient of composite ceramics was less than 5% in the temperature range of 25–115 °C, indicating that the $BaTiO_3$/Cu composite ceramics provided good stability in this temperature range. Therefore, these composites could be a novel temperature-stable dielectric material with a high ε_r. As for the steady rise in the permittivity between 115 and 130 °C, this could be due to the steady increase in space charge polarization (α_s) with temperature, which should be more than enough to offset the decrease due to the decrease in dipolar polarization (α_o)[7].

4. Conclusions

$BaTiO_3$/Cu composite ceramics without other secondary phases were prepared using a traditional solid-phase method in N_2 flow for 2 h at 1290 °C. The interface between $BaTiO_3$ and Cu will give an opportunity to develop an interpenetrating network with a strong ceramic–metal bonding. The conductivity of the $BaTiO_3$/Cu composite ceramics increased with increasing Cu content and followed the percolation theory with the percolation threshold of the $BaTiO_3$/Cu composite being at $x = 25$ wt.%. The permittivity increased as the amount of Cu increased and attained the value of ~9000 when $x = 30$ wt.%. Below the transition temperature (130 °C), the temperature coefficient of composite ceramics was less than 5% in the temperature range of 25–115 °C, and thus the ceramic would be a highly stable dielectric with high ε_r.

Acknowledgments

This research has been supported by the National Natural Science Foundation of China (51072106), Key Project of Chinese Ministry of Education (209126), Research projects of Science and Technology Division, Shaanxi (2010K10-14) and Foundation of Shaanxi Educational Committee (2010JK427).

References

[1] S. Panteny, C.R. Bowen, R. Stevens, Characterisation of barium titanate–silver composites. Part I. Microstructure and mechanical properties, J. Mater. Sci. 41 (2006) 3837–3843.
[2] J.F. Li, T. Kenta, T. Noriaki, Electrical and mechanical properties of piezoelectric ceramic/metal composites in the Pb(Zr,Ti)O_3/Pt system, J. Appl. Phys. Lett. 79 (2001) 2441–2443.
[3] S. Yoon, J. Dornseiffer, T. Schneller, et al., Percolative $BaTiO_3$–Ni composite nanopowders from alkoxide-mediated synthesis, J. Eur. Ceram. Soc. 30 (2010) 561–567.
[4] Y.F. Qu, Z.M. He, J.M. Ma, Study of Cr/PTC ceramics composite, J. Piezoelectrics Acoustooptics 22 (1) (2000) 33–36.
[5] W.C. Won, K. Isao, I.K. Ken, et al., Frequency dependence of dielectric properties of metallodielectric $SrTiO_3$–Pt composites, J. Eur. Ceram. Soc. 27 (2007) 2907–2910.
[6] H.J. Hwang, T. Nagai, T. Ohji, M. Sando, Curie temperature anomaly in lead zirconate titanate/silver composites, J. Am. Ceram. Soc. 81 (3) (1998) 709–712.
[7] C. Pecharroman, F.E. Betegon, J.F. Eartolome, et al., New percolative $BaTiO_3$–Ni composites with a high and frequency-independent dielectric constant ($\xi_r = 80{,}000$), J. Adv. Mater. 13 (20) (2001) 1541–1544.
[8] C.Y. Chen, W.H. Tuan, Effect of silver on the sintering and grain-growth behavior of barium titanate, J. Am. Ceram. Soc. 83 (12) (2000) 2988–2992.
[9] R. Sivakumar, T. Nishikawa, S. Honda, H. Awaji, F.D. Gnanam, Processing of mullite–molybdenum graded hollow cylinders by centrifugal molding technique, J. Eur. Ceram. Soc. 23 (2003) 765–772.
[10] M. Diaz, J.F. Bartolome, J. Requena, J.S. Moya, Wet processing of mullite/molybdenum composites, J. Eur. Ceram. Soc. 20 (2000) 1907–1914.
[11] J.F. Bartolome, M. Diaz, J. Requena, J.S. Moya, A.P. Tomsia, Mullite/molybdenum ceramic–metal composites, J. Acta Mater. 47 (1999) 3891–3899.

[12] C. Pecharroman, J.S. Moya, Experimental evidence a giant capacitance in insulator–conductor composites at percolation threshold, J. Adv. Mater. 12 (4) (2000) 294–297.
[13] Z. Chen, J.Q. Huang, C. Chen, G. Song, W. Han, P.Y. Du, Apercolative ferroelectric metal composite with hybrid dielectric dependence, J. Scripta Mater. 57 (2007) 921–924.
[14] E.S. Lopez, J.F. Bartolomea, C. Pecharromana, J.S. Moya, Wet processing and characterization of ZrO_2/stainless steel composites: electrical and mechanical performance, J. Mater. Res. Soc. 4 (2001) 217–222.
[15] W.H. Tzing, W.H. Tuan, H.L. Lin, The effect of microstructure on the electrical properties of NiO-doped $BaTiO_3$, Ceram. Int. 25 (1999) 425–430.
[16] W.H. Tzing, W.H. Tuan, Effect of NiO addition on the sintering and grain growth behaviors of $BaTiO_3$, Ceram. Int. 25 (1999) 69–75.
[17] M. Dietrich, F. Theo, Mechanical Properties, Failure Behaviour, Materials Selection, 2nd ed., Springer-Verlag, Berlin Heidelberg, New York, 2001.
[18] F.P. Glasser, in: B.S. Somiya (Ed.), Advances in the Performance of Cement-based Systems, Advanced Ceramics, Elsevier Science Publishers Ltd., 1990, pp. 157–161.
[19] D.H. Clyde, On crack direction in relation to Griffith's bi-axial failure criterion, J. Cem. Concrete Res. 3 (5) (1973) 537–547.
[20] J.I. Beltran, S. Gallego, J. Cerda, Oxygen vacancies at Ni/c-ZrO_2 interfaces Munoz MC, J. Eur. Ceram. Soc. 23 (2003) 2737–2740.
[21] E.S. Lopez, J.F. Bartolome, J.S. Moya, T. Tanimoto, Mechanical performance of 3Y-TZP/Ni composites: tensile, bending, and uniaxial fatigue tests, J. Mater. Res. 17 (2002) 1592–1600.
[22] C.W. Nan, Physics of inhomogeneous inorganic materials, J. Prog. Mater. Sci. 37 (1) (1993) 1–116.
[23] C.W. Nan, X.Z. Chen, Percolation model of Ti–Al_2O_3 cement, J. Acta Phys. Sci. 36 (4) (1987) 511–513.
[24] V. Singh, A.N. Tiwari, A.R. Kulkarni, Electrical behaviour of attritor processed Al/PMMS composite, J. Mater. Sci. Eng. B 41 (3) (1996) 310–313.
[25] M.S. Ardi, W. Dick, Dielectric properties of epoxy-barium titanate–carbon black composites, J. Rubber Compos. Process. Appl. 24 (3) (1995) 157–164.
[26] L.C. Costa, F. Henry, M.A. Valente, Electrical and dielectric properties of the percolating system polystyrene/polypyrrole particles, J. Eur. Polym. 38 (8) (2002) 1495–1499.
[27] H. Hyuga, Y. Hayashi, T. Sekino, Fabrication process and electrical properties of $BaTiO_3$/Ni nanocomposites, J. Nanostruct. Mater. 9 (1-8) (1997) 547–550.
[28] K. Konopka, A.O. Myalska, M. Szafram, Ceramic–metal composites with an interpenetrating network, Mater. Chem. Phys. 81 (2–3) (2003) 329–332.